 CMES, vol.17, no.3, pp.205-214, 2007

Contact Problem for the Flat Elliptical Crack under Normally Incident Shear Wave

A.N. Guz[1], O.V. Menshykov[1,2], V.V. Zozulya[3] and I.A. Guz [2]

Abstract: The contact interaction of opposite faces of an elliptical crack is studied for the case of a normal time-harmonic shear wave loading. The distribution of stress intensity factors (shear modes II and III) as functions of the wave number and the friction coefficient is investigated. The results are compared with those obtained for an elliptical crack without allowance for the contact interaction.

Keyword: Fracture mechanics; Cracked solid; Harmonic loading; Crack faces contact interaction.

1 Introduction

The rapid development of different areas of engineering, creation of new structures, modern problems of geophysics and seismology, make the computational fracture mechanics a topical area.

Among the most topical applied problems there are structural strength problems, complicated by the various flaws (cracks, delaminations, etc). Such flaws appear due to the process of manufacture of materials and structural components, and their further exploitation under various types of loading. The sudden development of cracks can lead to catastrophic aftereffects; therefore a considerable body of work is devoted to the solution of two- and three-dimensional fracture mechanics problems for cracked solids under dynamic loading, see Aliabadi and Rooke (1991), Aliabadi (2002), Atluri and Nishioka (1986), Balas, Sladek and Sladek (1989), Chen and Sih (1977), Cherepanov (1979), Domingez (1993), Freund (1990), Graff (1991), Guz and Zozulya (2002), Zhang and Gross (1998).

However it should be taken into account that during deformation of a solid, the opposite faces of cracks mutually interact with the unilateral contact forces in the normal direction and the frictional contact forces in the tangential direction. The contact zones, and the adhesion and sliding sub-zones appear on the faces of cracks. The boundaries between contact and non-contact zones, and also between adhesion and slipping sub-zones, are time dependant and unknown beforehand. It implies the significant transformation of the stress-strain state in the vicinity of crack front and the corresponding modification of the stress intensity factors distribution. The complexity of the problem is further compounded by the fact that the contact behaviour is very sensitive to the material properties of two contacting surfaces and the type of the external loading. Such dependences make the contact crack problem highly non-linear [Guz and Zozulya (2002)].

It is only possible to solve these problems using the advanced numerical methods, since the analytical solutions are limited to a relatively small number of idealized model problems corresponding to very special geometrical configurations and loading conditions. Some approaches and iterative algorithms based on the variational principles of the dynamic theory of elasticity were considered by Guz and Zozulya (2002), Mistakidis and Stavroulakis (1998), Zozulya and Menshykov (2003)]. Usually such problems are solved numerically using the finite element or boundary integral equations methods [Aliabadi and Rooke (1991), Aliabadi (2002), Atluri and Nish-

[1] Timoshenko Institute of Mechanics, National Academy of Sciences of Ukraine, Kiev, Ukraine.

[2] Centre for Micro- and Nanomechanics, School of Engineering and Physical Sciences, University of Aberdeen, Scotland, UK.

[3] Centro de Investigation Cientifica de Yucatan, Merida, Yucatan, México.

ioka (1986), Balas, Sladek and Sladek (1989), Domingez (1993), Zhang and Gross (1998). The boundary integral equations method is more preferable in the dynamic 3-D problems with changing boundary conditions, because this approach requires a relatively simple discretization of the surface rather than the volume, and offers the accuracy that is necessary for the computation of mechanical quantities such as stress intensity factors. However, the evaluation of divergent integrals with different types of singularity constitutes a major problem within the method. These integrals are often hyper-singular and should be treated in the sense of the Hadamard finite part [Guz and Zozulya (2002), Martin, Rizzo and Gonzalves (1989), Zozulya and Men'shikov (2000)].

It is important to point out, that in the majority of publications on fracture dynamics (except for our studies), problems were solved without taking into account the possibility of the contact interaction, though in dynamical problems it is almost impossible to find type of loading which do not cause crack faces contact interaction. The reviews of the results obtained for cracked solids with and without accounting for the contact interaction are given by Aliabadi and Rooke (1991), Aliabadi (2002), Balas, Sladek and Sladek (1989), Cherepanov (1979), Freund (1990), Graff (1991), Guz and Zozulya (2002), Zhang and Gross (1998), Men'shikov, Men'shikova and Wendland (2005).

The present paper is devoted to the solution of the three-dimensional fracture dynamics problem for a plane elliptical crack under a normally incident shear wave. The problem is solved with allowance for the contact interaction of the crack faces. The tangential forces, corresponding displacements of the crack faces and their effect on the distribution of stress intensity factors for different values of the friction coefficient are investigated.

2 Statement of the problem

Consider a plane stationary elliptical crack with a major axis a and a minor axis b located in the unbounded linear elastic, homogeneous and isotropic three-dimensional solid. The middle surface of the crack is defined by the following Cartesian coordinates:

$$\Omega = \left\{ \begin{array}{l} 0 \le x_1 \le a\cos\beta,\ 0 \le x_2 \le b\sin\beta, \\ x_3 = 0,\ \beta = \tan^{-1}(a/b\tan\varphi), \\ 0 \le \varphi < 2\pi,\ a \ge b \end{array} \right\}. \tag{1}$$

A time-harmonic shear SV-wave with the frequency ω and amplitude Φ_0 propagates normally to the crack surface. The shear axis coincides with the axis Ox_1 (Fig. 1).

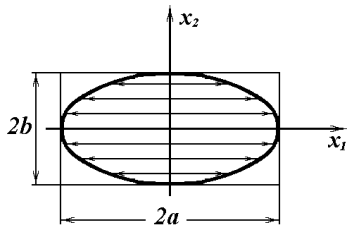

Figure 1: Elliptical crack under shear wave

The load vector on the crack faces can be represented as

$$\boldsymbol{p}(\boldsymbol{x},t) = p^*(\boldsymbol{x},t) + \boldsymbol{q}(\boldsymbol{x},t), \tag{2}$$

where $\boldsymbol{p}^*(\boldsymbol{x},t)$ is the load on the crack faces caused by the incident wave and $\boldsymbol{q}(\boldsymbol{x},t)$ is the contact force vector caused by the crack faces contact interaction. The displacement discontinuity vector $\Delta\boldsymbol{u}(\boldsymbol{x},t)$ characterizes the mutual displacement of the opposite crack faces.

According to Guz and Zozulya (2002), Guz, Zozulya and Men'shikov (2004), the following unilateral constraints must be fulfilled for the tangential components of the contact force vector and the displacement discontinuity vector:

$$\begin{aligned} &|\boldsymbol{q}_\tau(\boldsymbol{x},t)| < k_\tau q_n(\boldsymbol{x},t) \Rightarrow \partial_t \Delta\boldsymbol{u}_\tau(\boldsymbol{x},t) = 0; \\ &|\boldsymbol{q}_\tau(\boldsymbol{x},t)| = k_\tau q_n(\boldsymbol{x},t) \Rightarrow \partial_t \Delta\boldsymbol{u}_\tau(\boldsymbol{x},t) = -\lambda_\tau \boldsymbol{q}_\tau(\boldsymbol{x},t), \end{aligned} \tag{3}$$

where $\lambda_\tau = |\partial_t \Delta\boldsymbol{u}_\tau(\boldsymbol{x},t)|/|\boldsymbol{q}_\tau|$, and $k_\tau > 0$ is the friction coefficient, $q_n(\boldsymbol{x},t)$ is the normal component of the contact force vector. In order to take the unilateral constraints (3) into account, we assume that $q_n(\boldsymbol{x},t)$ is the unit constant in the considered model case.

The constraints (3) mean that the friction is described by the Coulomb law. The opposite crack faces remain immovable to each other in the tangential plane until they are held by the friction force. However, as soon as the magnitude of the contact forces reaches a certain limit, depending on the friction coefficient and exceeds this limit, the crack faces begin to move: the slipping occurs.

3 Boundary integral equations

Since the area of the contact domain Ω_{cont} is time-dependent, we can expand the components of the load and displacement discontinuity vectors into the Fourier series [Guz and Zozulya (2002), Guz, Menshykov and Zozulya (2003)]:

$$p_j(\boldsymbol{x},t) = \mathrm{Re}\left\{\sum_{k=-\infty}^{+\infty} p_j^k(\boldsymbol{x}) e^{i\omega_k t}\right\}, \tag{4}$$

$$\Delta u_j(\boldsymbol{x},t) = \mathrm{Re}\left\{\sum_{k=-\infty}^{+\infty} \Delta u_j^k(\boldsymbol{x}) e^{i\omega_k t}\right\}, \tag{5}$$

where $\omega_k = 2\pi k/T$, $j = 1,2$ and

$$p_j^k(\boldsymbol{x}) = \frac{\omega}{2\pi}\int_0^T p_j(\boldsymbol{x},t) e^{-i\omega_k t} dt, \tag{6}$$

$$\Delta u_j^k(\boldsymbol{x}) = \frac{\omega}{2\pi}\int_0^T \Delta u_j(\boldsymbol{x},t) e^{-i\omega_k t} dt. \tag{7}$$

The Fourier coefficients $p_j^k(\boldsymbol{x})$ and $\Delta u_j^k(\boldsymbol{x})$ are related by the following system of boundary integral equations for $k = \overline{-\infty,+\infty}$

$$p_1^k(\boldsymbol{x}) = -\int_\Omega F_{11}(\boldsymbol{x},\boldsymbol{y},\omega_k)\Delta u_1^k(\boldsymbol{y})d\boldsymbol{y} - \int_\Omega F_{12}(\boldsymbol{x},\boldsymbol{y},\omega_k)\Delta u_2^k(\boldsymbol{y})d\boldsymbol{y}, \tag{8}$$

$$p_2^k(\boldsymbol{x}) = -\int_\Omega F_{21}(\boldsymbol{x},\boldsymbol{y},\omega_k)\Delta u_1^k(\boldsymbol{y})d\boldsymbol{y} - \int_\Omega F_{22}(\boldsymbol{x},\boldsymbol{y},\omega_k)\Delta u_2^k(\boldsymbol{y})d\boldsymbol{y}. \tag{9}$$

Taking into account the Euler formula

$$e^{a+ib} = e^a(\cos(b) + i\sin(b)), \tag{10}$$

we obtain the expressions for the Fourier coefficients (6), (7):

$$p_j^k(\boldsymbol{x}) = \frac{\omega}{2\pi}\int_0^T p_j(\boldsymbol{x},t)\cos(\omega_k t)dt - i\frac{\omega}{2\pi}\int_0^T p_j(\boldsymbol{x},t)\sin(\omega_k t)dt, \tag{11}$$

$$\Delta u_j^k(\boldsymbol{x}) = \frac{\omega}{2\pi}\int_0^T \Delta u_j(\boldsymbol{x},t)\cos(\omega_k t)dt - i\frac{\omega}{2\pi}\int_0^T \Delta u_j(\boldsymbol{x},t)\sin(\omega_k t)dt. \tag{12}$$

Let us denote

$$p_{j,\cos}^k(\boldsymbol{x}) = \frac{\omega}{\pi}\int_0^T p_j(\boldsymbol{x},t)\cos(\omega_k t)dt, \tag{13}$$

$$p_{j,\sin}^k(\boldsymbol{x}) = \frac{\omega}{\pi}\int_0^T p_j(\boldsymbol{x},t)\sin(\omega_k t)dt, \tag{14}$$

$$\Delta u_{j,\cos}^k(\boldsymbol{x}) = \frac{\omega}{\pi}\int_0^T \Delta u_j(\boldsymbol{x},t)\cos(\omega_k t)dt, \tag{15}$$

$$\Delta u_{j,\sin}^k(\boldsymbol{x}) = \frac{\omega}{\pi}\int_0^T \Delta u_j(\boldsymbol{x},t)\sin(\omega_k t)dt, \tag{16}$$

then

$$p_j(\boldsymbol{x},t) = \frac{p_{j,\cos}^0(\boldsymbol{x})}{2} + \sum_{m=1}^{+\infty}\left(p_{j,\cos}^k(\boldsymbol{x})\cos(\omega_k t) + p_{j,\sin}^k(\boldsymbol{x})\sin(\omega_k t)\right), \tag{17}$$

$$\Delta u_j(\boldsymbol{x},t) = \frac{\Delta u_{j,\cos}^0(\boldsymbol{x})}{2} + \sum_{k=1}^{+\infty}\left(\Delta u_{j,\cos}^k(\boldsymbol{x})\cos(\omega_k t) + \Delta u_{j,\sin}^k(\boldsymbol{x})\sin(\omega_k t)\right). \tag{18}$$

The boundary integral system of equations (8), (9) for $k=\overline{0,+\infty}$ takes the form:

$$p^k_{1,\cos}(\boldsymbol{x})-ip^k_{1,\sin}(\boldsymbol{x})= -\sum_{j=1}^{2}\int_{\Omega}(F^{Re}_{1j}(\boldsymbol{x},\boldsymbol{y},\omega_k)+iF^{Im}_{1j}(\boldsymbol{x},\boldsymbol{y},\omega_k)) \times(\Delta u^k_{j,\cos}(\boldsymbol{y})-i\Delta u^k_{j,\sin}(\boldsymbol{y}))\,d\boldsymbol{y}, \quad (19)$$

$$p^k_{2,\cos}(\boldsymbol{x})-ip^k_{2,\sin}(\boldsymbol{x})= -\sum_{j=1}^{2}\int_{\Omega}(F^{Re}_{2j}(\boldsymbol{x},\boldsymbol{y},\omega_k)+iF^{Im}_{2j}(\boldsymbol{x},\boldsymbol{y},\omega_k)) \times(\Delta u^k_{j,\cos}(\boldsymbol{y})-i\Delta u^k_{j,\sin}(\boldsymbol{y}))\,d\boldsymbol{y}, \quad (20)$$

where $F^{Re}_{ij}(\boldsymbol{x},\boldsymbol{y},\omega_k)$ and $F^{Im}_{ij}(\boldsymbol{x},\boldsymbol{y},\omega_k)$ are the real and imaginary components of the fundamental solution $F_{ij}(\boldsymbol{x},\boldsymbol{y},\omega_k)$, which can be determined from the Green displacement tensor. For a flat crack we have [Guz, Zozulya and Men'shikov (2004), Menshykov and Guz (2006, 2007)]:

$$\begin{aligned}F_{11}&=\frac{1}{r^3}\frac{\mu}{4\pi(\lambda+2\mu)}\left[3\lambda\frac{(y_1-x_1)^2}{r^2}+2\mu\right]\\&-\frac{1}{r^3}\frac{\mu}{4\pi}\left\{\frac{(y_1-x_1)^2}{r^2}\right.\\&\cdot\sum_{n=3}^{+\infty}\left[\frac{(-l_2)^n}{n!}\frac{(n-1)(n-2)(n-3)}{(n+2)}\right.\\&\left.+\frac{(-l_1)^n}{n!}\frac{c_2^2}{c_1^2}\frac{4(n-1)(n-2)}{(n+2)}\right]\\&+2\sum_{n=2}^{+\infty}\left[\frac{(-l_2)^n}{n!}\frac{n(n-1)}{(n+2)}\right.\\&\left.\left.+\frac{(-l_1)^n}{n!}\frac{c_2^2}{c_1^2}\frac{2(n-1)}{(n+2)}\right]\right\},\end{aligned} \quad (21)$$

$$\begin{aligned}F_{22}&=\frac{1}{r^3}\frac{\mu}{4\pi(\lambda+2\mu)}\left[3\lambda\frac{(y_2-x_2)^2}{r^2}+2\mu\right]\\&-\frac{1}{r^3}\frac{\mu}{4\pi}\left\{\frac{(y_2-x_2)^2}{r^2}\right.\\&\cdot\sum_{n=3}^{\infty}\left[\frac{(-l_2)^n}{n!}\frac{(n-1)(n-2)(n-3)}{(n+2)}\right.\\&\left.+\frac{(-l_1)^n}{n!}\frac{c_2^2}{c_1^2}\frac{4(n-1)(n-2)}{(n+2)}\right]\\&+2\sum_{n=2}^{\infty}\left[\frac{(-l_2)^n}{n!}\frac{n(n-1)}{(n+2)}\right.\\&\left.\left.+\frac{(-l_1)^n}{n!}\frac{c_2^2}{c_1^2}\frac{2(n-1)}{(n+2)}\right]\right\},\end{aligned} \quad (22)$$

$$\begin{aligned}F_{12}=F_{21}&=\frac{1}{r^3}\frac{3\lambda\mu}{4\pi(\lambda+2\mu)}\frac{(y_1-x_1)(y_2-x_2)}{r^2}\\&-\frac{1}{r^3}\frac{\mu}{4\pi}\frac{(y_1-x_1)(y_2-x_2)}{r^2}\times\\&\sum_{n=3}^{\infty}\left[\frac{(-l_2)^n}{n!}\frac{(n-1)(n-2)(n-3)}{(n+2)}\right.\\&\left.+\frac{(-l_1)^n}{n!}\frac{c_2^2}{c_1^2}\frac{4(n-1)(n-2)}{(n+2)}\right],\end{aligned} \quad (23)$$

where $l_1=i\omega_k r/c_1$, $l_2=i\omega_k r/c_2$; r is the distance between the observation point and the point of application of the load; $c_1=\sqrt{(\lambda+2\mu)/\rho}$ and $c_2=\sqrt{\mu/\rho}$ are the velocities of the longitudinal and the transverse waves; $\lambda>-\mu$ and $\mu>0$ are the Lame elastic constants; ρ is the material density.

Note that the number of retained terms in the series (21)–(23) required for evaluating of these series with a fixed accuracy increases with a rise in the frequency ω. Therefore the speed of convergence decreases. It can result in aggravation of the accuracy of the numerical solution. In particular, it is not possible to consider the limit case in which $\omega\to+\infty$.

We approximate the surface of the crack by a set of plane elements $\Omega^h_l, l=\overline{1,N}$, and use a piecewise constant approximation of the known and unknown functions. Thus, we obtain from the

system of boundary integral equations (19), (20) for $k = \overline{0,+\infty}$ the following system of complex-valued equations:

$$p^k_{1,\cos}(\mathbf{x}_m) - ip^k_{1,\sin}(\mathbf{x}_m) = -\sum_{j=1}^{2}\sum_{l=1}^{N}\int\limits_{\Omega^h_l}(F^{Re}_{1j}(\mathbf{x}_m,\mathbf{y},\omega_k)+iF^{Im}_{1j}(\mathbf{x}_m,\mathbf{y},\omega_k))d\mathbf{y} \times (\Delta u^k_{j,\cos}(\mathbf{y}_l) - i\Delta u^k_{j,\sin}(\mathbf{y}_l)), \quad (24)$$

$$p^k_{2,\cos}(\mathbf{x}_m) - ip^k_{2,\sin}(\mathbf{x}_m) = -\sum_{j=1}^{2}\sum_{l=1}^{N}\int\limits_{\Omega^h_l}(F^{Re}_{2j}(\mathbf{x}_m,\mathbf{y},\omega_k)+iF^{Im}_{2j}(\mathbf{x}_m,\mathbf{y},\omega_k))d\mathbf{y} \times (\Delta u^k_{j,\cos}(\mathbf{y}_l) - i\Delta u^k_{j,\sin}(\mathbf{y}_l)), \quad (25)$$

where points $\mathbf{x}_j$ and $\mathbf{y}_j$ are located in the centre of element Ω^h_j. The matrix form of the system of equations (24), (25) can be found in Appendix A.

Due to the presence of non-integrable singularities in the integral kernels $F_{ij}(\boldsymbol{x},\boldsymbol{y},\omega_k)$, whose rank exceeds the dimension of the integration region, the integrals included in the system of boundary integral equations (19), (20) are hypersingular. We should treat them only in the sense of the Hadamard finite parts. Guz and Zozulya (2002), Zozulya and Men'shikov (2000) give the relationships enabling us to calculate the divergent integrals. The corresponding regularized expressions are given in Appendix B.

4 Numerical results

Let the incident shear wave with the unit amplitude propagate in the material with the following mechanical properties: the Young's elastic modulus $E = 200\ GPa$, the Poisson's ratio $\nu = 0.25$, the density $\rho = 7800\ kg/m^3$.

Here the iterative algorithm [Guz and Zozulya (2002), Mistakidis and Stavroulakis (1998), Zozulya and Menshykov (2003)] is used for solving the problem. It consists of the following steps:

- assigning an initial distribution of the traction vector $\boldsymbol{p}(\boldsymbol{x},t) = \boldsymbol{p}^*(\boldsymbol{x},t) = (\mathrm{Re}(-\mu k_2^2\Phi_0 e^{-i\omega t}),0,0)^T$ on the crack faces;
- solving the problem without taking the contact interaction into account;
- correcting the distribution of the contact forces vector and the displacement discontinuity vector by using the operators of orthogonal projection on the set determined by constraints (3);
- proceeding to the next iteration until no additional correction is needed.

The distribution of the tangential components of the contact forces and the displacement discontinuity vectors for a penny-shaped crack ($a/b = 1.0$) is given in Fig. 2.

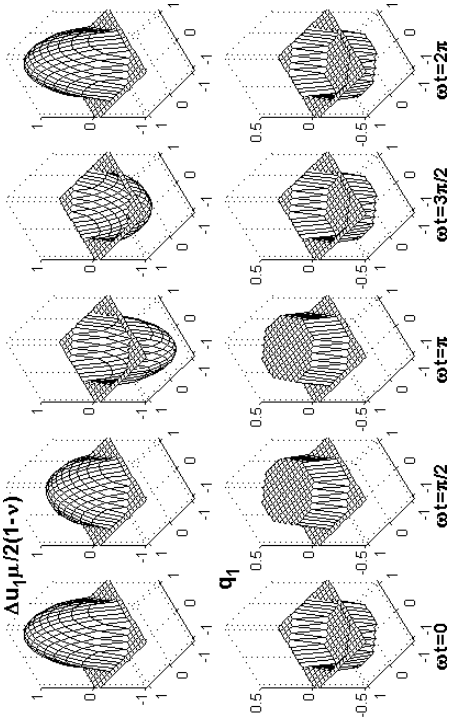

Figure 2: Tangential contact forces and normalized displacement discontinuity on the surface of the crack, $k_2 a = 1.0$; $k_\tau = 0.3$

Note that the constraints (3) are satisfied on the entire surface of the crack during the period of oscillations. Also the distribution of the tangential components has a relatively simple form only by the virtue of the assumption about the constant distribution of the normal component of contact

forces. Otherwise, the distribution of the tangential components would have a significantly more complicated form.

The following asymptotic formulas [Cherepanov (1979), Guz and Zozulya (2002)] were applied to calculate the stress intensity factors:

$$K_{II}(\mathbf{x},t) = \lim_{r\to 0} \frac{\mu}{4(1-\nu)} \sqrt{\frac{2\pi}{r}} \Delta u_\tau^n(\mathbf{x},t), \tag{26}$$

$$K_{III}(\mathbf{x},t) = \lim_{r\to 0} \frac{\mu}{4} \sqrt{\frac{2\pi}{r}} \Delta u_\tau^\tau(\mathbf{x},t), \tag{27}$$

where $\Delta u_\tau^n(\mathbf{x},t)$, $\Delta u_\tau^\tau(\mathbf{x},t)$ are the normal and tangential components of vector $\Delta \boldsymbol{u}_\tau(\mathbf{x},t)$ in the vicinity of the crack front; r is the distance from the crack front.

The stress intensity factor $K_{II}(\boldsymbol{x},t)$ attains the maximum value in the vertex of the major axis of the ellipse ($\beta = 0^0$), the minimum value - in the vertex of the minor axis ($\beta = 90^0$). The opposite is true for the factor $K_{III}(\boldsymbol{x},t)$. The values of the stress intensity factors are shown in Fig. 3-6, where the dimensionless parameters $\left|K_{II}^{\max}/K_{II}^{\text{stat}}\right|$ and $\left|K_{III}^{\max}/K_{III}^{\text{stat}}\right|$ are given for $\beta = 0^0$ and $\beta = 90^0$. Here K_{II}^{stat} and K_{III}^{stat} are the corresponding static values determined for a penny-shaped crack from the relationships [Cherepanov (1979), Gross and Zhang (1992)]:

$$K_{II}^{\text{stat}} = \frac{4}{\sqrt{\pi}(2-\nu)} \tau \sqrt{a} \cos\beta, \tag{28}$$

$$K_{III}^{\text{stat}} = -\frac{4(1-\nu)}{\sqrt{\pi}(2-\nu)} \tau \sqrt{a} \sin\beta, \tag{29}$$

and for an elliptical crack from the relationships [Chen and Sih (1977), Cherepanov (1979), Kassier and Sih (1966)]:

$$K_{II}^{\text{stat}} = -\frac{\sqrt{\pi}}{(ab)^{3/2}\Pi^{1/4}} bB\cos\beta, \tag{30}$$

$$K_{III}^{\text{stat}} = \frac{\sqrt{\pi}(1-\nu)}{(ab)^{3/2}\Pi^{1/4}} aB\sin\beta, \tag{31}$$

$$\Pi = a^2\sin^2\beta + b^2\cos^2\beta, \tag{32}$$

$$B = -\frac{ab^2k^2\tau}{(k^2-\nu)E(k) + \nu k' K(k)}, \tag{33}$$

$$k^2 = 1 - b^2/a^2, \quad k' = b/a, \quad b < a, \tag{34}$$

where τ denotes the stress amplitude of the incident wave. $K(k)$ and $E(k)$ are the complete normal Legendre elliptic integrals:

$$K(k) = \int_0^{\pi/2} \frac{d\theta}{\sqrt{1-k^2\sin^2\theta}}, \tag{35}$$

$$E(k) = \int_0^{\pi/2} \sqrt{1-k^2\sin^2\theta}\, d\theta. \tag{36}$$

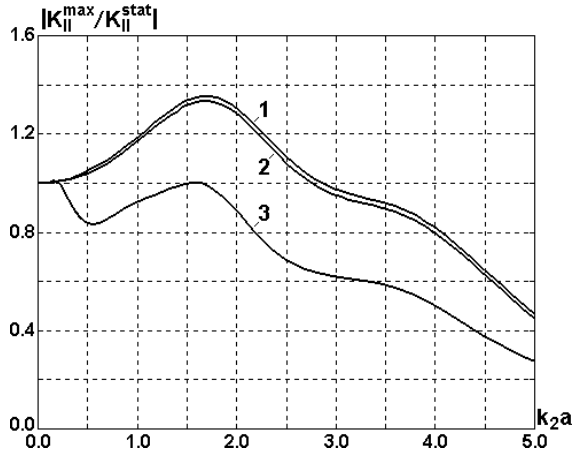

Figure 3: Dimensionless stress intensity factor $|K_{II}^{\max}/K_{II}^{stat}|$ plotted against the wave number k_2a; $a/b = 1.0$: 1 -without contact; 2 - $k_\tau = 0.02$; 3 - $k_\tau = 0.3$

The stress intensity factors diminish with the rise in the friction coefficient. As k_τ tends to zero the solution tends to the one obtained without allowance for the contact interaction (Fig. 3–6, curves 1 and 2). For the larger values of the friction coefficient the stress intensity factors reach the maximum values when the wave numbers are close to zero (Fig. 3–6, curves 3).

The results obtained for the penny-shaped crack with the neglected effect of contact interaction coincide with the results of Gross and Zhang (1992), Zhang and Gross (1998) in the range $0.0 \le k_2a \le 4.0$, and only insignificantly differ from them in the range $4.0 \le k_2a \le 5.0$. It can be associated with the mentioned aggravation of the precision of the solution with the increasing of frequency.

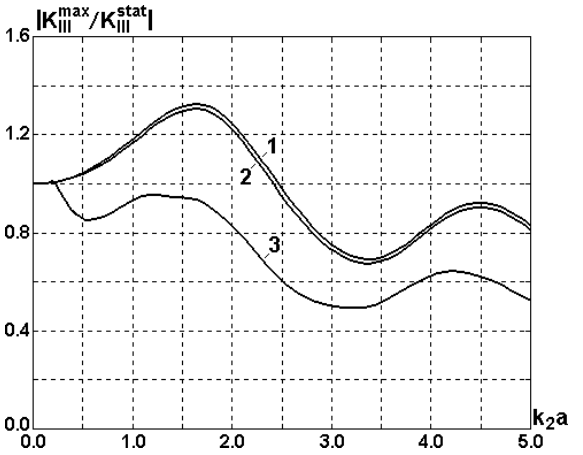

Figure 4: Dimensionless stress intensity factor $|K_{III}^{\max}/K_{III}^{stat}|$ plotted against the wave number k_2a; $a/b = 1.0$: 1 -without contact; 2 - $k_\tau = 0.02$; 3 - $k_\tau = 0.3$

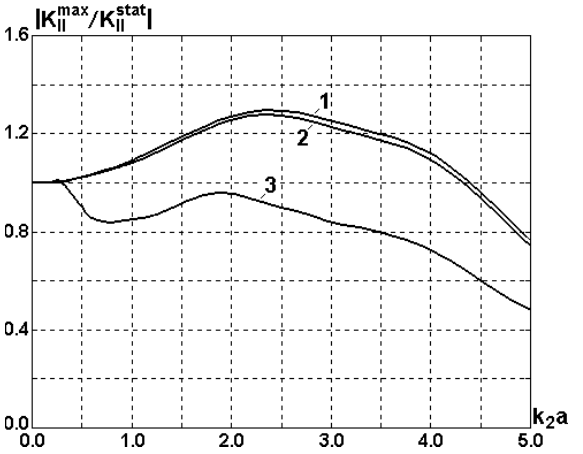

Figure 5: Dimensionless stress intensity factor $|K_{II}^{\max}/K_{II}^{stat}|$ plotted against the wave number k_2a; $a/b = 2.0$: 1 -without contact; 2 - $k_\tau = 0.02$; 3 - $k_\tau = 0.3$

5 Conclusions

In this paper the distribution of stress intensity factors (shear modes) was investigated for the case of a flat elliptical crack in the unbounded linear elastic, homogeneous and isotropic three-dimensional solid under time-harmonic shear wave, propagating normally to the crack surface. The problem was solved by the boundary integral equations methods using an iterative algorithm. The effect of the friction was analyzed, where

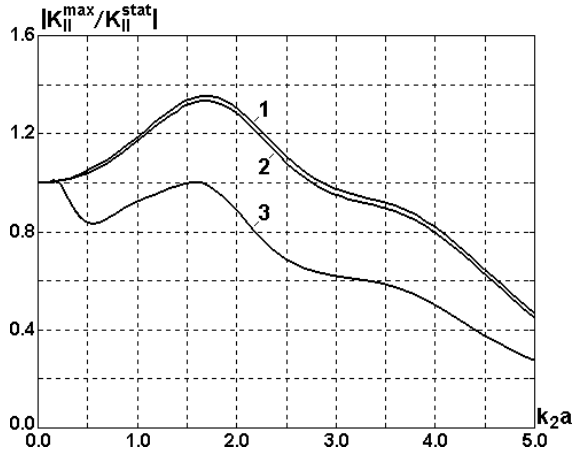

Figure 6: Dimensionless stress intensity factor $|K_{III}^{\max}/K_{III}^{stat}|$ plotted against the wave number k_2a; $a/b = 2.0$: 1 -without contact; 2 - $k_\tau = 0.02$; 3 - $k_\tau = 0.3$

friction was described by the Coulomb law.

The stress intensity factors were given as functions of the wave number and the friction coefficient. The location of the maximum values of the stress intensity factors was defined. The results are compared with those obtained without allowance for the contact interaction. It was shown that in some cases the difference between compared results can reach 50%.

The results presented here confirm the significance of taking into account the contact interaction of crack faces. Hence, additional extensive investigations are necessary to ensure safety of structures.

References

Aliabadi, M.H.; Rooke, D.P. (1991): *Numerical Fracture Mechanics*, Computational Mechanics Publications, Boston, Kluwer Academic Publishers, Dordrecht, Boston, London.

Aliabadi, M.H. (2002) The Boundary Element Method: Application in Solids and Structures. In: L.C. Wrobel, M.H. Aliabadi (eds) *The Boundary Element Method*, John Wiley & Sons Inc.

Atluri, S.N.; Nishioka, T. (1986): Computational Methods for Three-Dimensional Problems of Fracture. In: S.N. Atluri (ed) *Computational*

methods in the mechanics of fracture, Elsevier, Amsterdam, pp. 228–291.

Balas J., Sladek, J.; Sladek, V. (1989): Stress analysis by boundary element methods. Elsevier, Amsterdam.

Chen E.P.; Sih, G.C. (1977): Scattering waves about stationary and moving cracks. In: G.C. Sih (ed) *Mechanics of Fracture 4: Elastodynamic Crack Problems*, Noordhoff Intl. Publ., Leyden, pp. 119–212.

Cherepanov, G.P. (1979): Mechanics of brittle fracture. McGraw Hill, New York.

Domingez, J. (1993): Boundary Elements in Dynamics. Computational Mechanics Publications, Southampton.

Gross, D.; Zhang, Ch. (1992): Wave propagation in damaged solids. International Journal of Solids Structures, 29, pp. 1763–1779.

Freund, L.B. (1990): Dynamic fracture mechanics. Cambridge Uni. Press, NY.

Kassier, M.K.; Sih, G.C. (1966): Three-dimensional stress distribution around an elliptical crack under arbitrary loadings, Trans. ASME, ser. E, J. Appl. Mech. 33(3), pp. 601–611.

Martin P.A., Rizzo F.J., Gonzalves I.R. (1989) On hypersingular boundary integral equations for certain problems in mechanics. Mechanics Research Communications. 16, pp. 65–71.

Mistakidis, E.S.; Stavroulakis, G.E. (1998): Nonconvex optimization in mechanics. Algorithms, heuristics and engineering applications by FEM. Kluwer Academic Publishers.

Graff, K.F. (1991) Wave motion in elastic solids. Dover Publications, New York.

Guz, A.N.; Menshykov, O.V.; Zozulya, V.V. (2003): Surface contact of elliptical crack under normally incident tension-compression wave, Theoretical and Applied Fracture Mechanics, 40(3), pp. 285–291.

Guz, A.N.; Zozulya, V.V. (2002): Elastodynamic unilateral contact problems with friction for bodies with cracks, International Applied Mechanics, 38(8), 895–932.

Guz, A.N.; Zozulya, V.V.; Men'shikov, A.V. (2004): General spatial dynamic problem for an elliptic crack under the action of a normal shear wave, with consideration for the contact interaction of the crack faces, International Applied Mechanics, 40(2), pp. 156–159.

Men'shikov, A.V.; Men'shikova, M.V.; Wendland, W.L. (2005) On use the Galerkin method to solve the elastodynamic problem for a linear crack under normal loading. International Applied Mechanics, 41(11), pp. 1324–1329.

Menshykov, O.V.; Guz, I.A. (2006) Contact interaction of crack faces under harmonic loading at oblique incidence. International Journal of Fracture, 139, pp. 145–152.

Menshykov, O.V.; Guz, I.A. (2007) Effect of contact interaction of the crack faces for a crack under harmonic loading. International Applied Mechanics, 43(2): in press.

Zhang, Ch.; Gross, D. (1998): On wave propagation in elastic solids with cracks (Comp. Mech. Publ., Southampton, UK, Boston, USA).

Zozulya, V.V.; Men'shikov, V.A. (2000): Solutions of three-dimensional problems of the dynamic theory of elasticity for bodies with cracks using hypersingular integrals, International Applied Mechanics, 36(1), pp. 74–81.

Zozulya, V.V.; Menshykov, O.V. (2003): Use of the constrained optimization algorithms in some problems of fracture mechanics, Optimization and Engineering, 4(4), pp. 365–384.

Appendix A: Matrix form of the system of linear algebraic equations

After separation of the real and imaginary parts, the system of equations (24), (25) can be written in the following short matrix form:

$$\boldsymbol{F}_{\tau}^{k}\boldsymbol{U}_{\tau}^{k}=\boldsymbol{P}_{\tau}^{k}, \tag{A1.1}$$

where

$$\boldsymbol{F}_{\tau}^{k}=\begin{bmatrix}-\mathbf{F}_{11}^{k,Re} & -\mathbf{F}_{11}^{k,Im} & -\mathbf{F}_{12}^{k,Re} & -\mathbf{F}_{12}^{k,Im}\\ \mathbf{F}_{11}^{k,Im} & -\mathbf{F}_{11}^{k,Re} & \mathbf{F}_{12}^{k,Im} & -\mathbf{F}_{12}^{k,Re}\\ -\mathbf{F}_{21}^{k,Re} & -\mathbf{F}_{21}^{k,Im} & -\mathbf{F}_{22}^{k,Re} & -\mathbf{F}_{22}^{k,Im}\\ \mathbf{F}_{21}^{k,Im} & -\mathbf{F}_{21}^{k,Re} & \mathbf{F}_{22}^{k,Im} & -\mathbf{F}_{22}^{k,Re}\end{bmatrix},$$

$$\boldsymbol{U}_{\tau}^{k}=\begin{bmatrix}U_{1,\cos}^{k}\\ U_{1,\sin}^{k}\\ U_{2,\cos}^{k}\\ U_{2,\sin}^{k}\end{bmatrix},\quad \boldsymbol{P}_{\tau}^{k}=\begin{bmatrix}\mathbf{P}_{1,\cos}^{k}\\ \mathbf{P}_{1,\sin}^{k}\\ \mathbf{P}_{2,\cos}^{k}\\ \mathbf{P}_{2,\sin}^{k}\end{bmatrix}, \tag{A1.2}$$

and

$$\mathbf{F}_{qp}^{k,Re}=\begin{bmatrix}\int\limits_{\Omega_1^h}F_{qp}^{Re}(\mathbf{x}_1,\mathbf{y},\omega_k)d\mathbf{y} & \int\limits_{\Omega_2^h}F_{qp}^{Re}(\mathbf{x}_1,\mathbf{y},\omega_k)d\mathbf{y} & \cdots & \int\limits_{\Omega_N^h}F_{qp}^{Re}(\mathbf{x}_1,\mathbf{y},\omega_k)d\mathbf{y}\\ \int\limits_{\Omega_1^h}F_{qp}^{Re}(\mathbf{x}_2,\mathbf{y},\omega_k)d\mathbf{y} & \int\limits_{\Omega_2^h}F_{qp}^{Re}(\mathbf{x}_2,\mathbf{y},\omega_k)d\mathbf{y} & \cdots & \int\limits_{\Omega_N^h}F_{qp}^{Re}(\mathbf{x}_2,\mathbf{y},\omega_k)d\mathbf{y}\\ \vdots & \vdots & \ddots & \vdots\\ \int\limits_{\Omega_1^h}F_{qp}^{Re}(\mathbf{x}_N,\mathbf{y},\omega_k)d\mathbf{y} & \int\limits_{\Omega_2^h}F_{qp}^{Re}(\mathbf{x}_N,\mathbf{y},\omega_k)d\mathbf{y} & \cdots & \int\limits_{\Omega_N^h}F_{qp}^{Re}(\mathbf{x}_N,\mathbf{y},\omega_k)d\mathbf{y}\end{bmatrix}, \tag{A1.3}$$

$$\mathbf{F}_{qp}^{k,Im}=\begin{bmatrix}\int\limits_{\Omega_1^h}F_{qp}^{Im}(\mathbf{x}_1,\mathbf{y},\omega_k)d\mathbf{y} & \int\limits_{\Omega_2^h}F_{qp}^{Im}(\mathbf{x}_1,\mathbf{y},\omega_k)d\mathbf{y} & \cdots & \int\limits_{\Omega_N^h}F_{qp}^{Im}(\mathbf{x}_1,\mathbf{y},\omega_k)d\mathbf{y}\\ \int\limits_{\Omega_1^h}F_{qp}^{Im}(\mathbf{x}_2,\mathbf{y},\omega_k)d\mathbf{y} & \int\limits_{\Omega_2^h}F_{qp}^{Im}(\mathbf{x}_2,\mathbf{y},\omega_k)d\mathbf{y} & \cdots & \int\limits_{\Omega_N^h}F_{qp}^{Im}(\mathbf{x}_2,\mathbf{y},\omega_k)d\mathbf{y}\\ \vdots & \vdots & \ddots & \vdots\\ \int\limits_{\Omega_1^h}F_{qp}^{Im}(\mathbf{x}_N,\mathbf{y},\omega_k)d\mathbf{y} & \int\limits_{\Omega_2^h}F_{qp}^{Im}(\mathbf{x}_N,\mathbf{y},\omega_k)d\mathbf{y} & \cdots & \int\limits_{\Omega_N^h}F_{qp}^{Im}(\mathbf{x}_N,\mathbf{y},\omega_k)d\mathbf{y}\end{bmatrix}, \tag{A1.4}$$

$$\mathbf{U}_{q,\cos}^{k}=\begin{bmatrix}\Delta u_{q,\cos}^{k}(\mathbf{y}_1)\\ \Delta u_{q,\cos}^{k}(\mathbf{y}_2)\\ \cdots\\ \Delta u_{q,\cos}^{k}(\mathbf{y}_N)\end{bmatrix},\ \mathbf{U}_{q,\sin}^{k}=\begin{bmatrix}\Delta u_{q,\sin}^{k}(\mathbf{y}_1)\\ \Delta u_{q,\sin}^{k}(\mathbf{y}_2)\\ \cdots\\ \Delta u_{q,\sin}^{k}(\mathbf{y}_N)\end{bmatrix},$$

$$\mathbf{P}_{q,\cos}^{k}=\begin{bmatrix}p_{q,\cos}^{k}(\mathbf{y}_1)\\ p_{q,\cos}^{k}(\mathbf{y}_2)\\ \cdots\\ p_{q,\cos}^{k}(\mathbf{y}_N)\end{bmatrix},\quad \mathbf{P}_{q,\sin}^{k}=\begin{bmatrix}p_{q,\sin}^{k}(\mathbf{y}_1)\\ p_{q,\sin}^{k}(\mathbf{y}_2)\\ \cdots\\ p_{q,\sin}^{k}(\mathbf{y}_N)\end{bmatrix}. \tag{A1.5}$$

Appendix B: Regularization of divergent integrals

It follows from expressions (21)–(23) for the fundamental solutions $F_{ij}(\boldsymbol{x},\boldsymbol{y},\omega_k)$ that in order to calculate the coefficients of the system of equations (24), (25) the divergent integrals

$$J_{\gamma}^{\alpha,\beta}(\boldsymbol{x},\Omega_j^h)=\int\limits_{\Omega_j^h}\frac{(x_1-y_1)^{\alpha}(x_2-y_2)^{\beta}}{r^{\gamma}}d\mathbf{y} \tag{A2.1}$$

should be regularized and calculated over plane elements Ω_j^h, $j=\overline{1,N}$.

It was shown by Zozulya, Men'shikov (2000) that for regularization of the divergent integrals the second Green theorem can be used. Particularly, we obtain the following regular representations for weakly singular integrals

$$J_1^{0,0}(\boldsymbol{x},\Omega_j^h)=-\int\limits_{\partial\Omega_j^h}\left[\frac{x_1-y_1}{r}n_1(\boldsymbol{y})+\frac{x_2-y_2}{r}n_2(\boldsymbol{y})\right]d\boldsymbol{y}, \tag{A2.2}$$

$$J_3^{1,1}(\boldsymbol{x},\Omega_j^h)=\frac{1}{5}\int\limits_{\partial\Omega_j^h}\left[\frac{x_1-y_1}{r}n_2(\boldsymbol{y})+\frac{x_2-y_2}{r}n_1(\boldsymbol{y})-3\frac{(x_1-y_1)^2(x_2-y_2)}{r^3}n_1(\boldsymbol{y})-3\frac{(x_1-y_1)(x_2-y_2)^2}{r^3}n_2(\boldsymbol{y})\right]d\boldsymbol{y}, \tag{A2.3}$$

$$J_3^{2,0}(\boldsymbol{x},\Omega_j^h)=\frac{1}{5}\int\limits_{\partial\Omega_j^h}\left[-2\frac{x_2-y_2}{r}n_2(\boldsymbol{y})-3\frac{(x_1-y_1)^3}{r^3}n_1(\boldsymbol{y})-3\frac{(x_1-y_1)^2(x_2-y_2)}{r^3}n_2(\boldsymbol{y})\right]d\boldsymbol{y}, \tag{A2.4}$$

$$J_3^{0,2}(\boldsymbol{x},\Omega_j^h)=\frac{1}{5}\int\limits_{\partial\Omega_j^h}\left[-2\frac{x_1-y_1}{r}n_1(\boldsymbol{y})-3\frac{(x_2-y_2)^3}{r^3}n_2(\boldsymbol{y})-3\frac{(x_1-y_1)(x_2-y_2)^2}{r^3}n_1(\boldsymbol{y})\right]d\boldsymbol{y}, \tag{A2.5}$$

and for hypersingular integrals

$$J_3^{0,0}(\boldsymbol{x},\Omega_j^h) = \int\limits_{\partial\Omega_j^h} \left[\frac{x_1-y_1}{r^3}n_1(\boldsymbol{y}) + \frac{x_2-y_2}{r^3}n_2(\boldsymbol{y})\right] d\boldsymbol{y}, \quad \text{(A2.6)}$$

$$J_5^{1,1}(\boldsymbol{x},\Omega_j^h) = \frac{1}{5}\int\limits_{\partial\Omega_j^h} \left[\frac{x_1-y_1}{r^3}n_2(\boldsymbol{y}) + \frac{x_2-y_2}{r^3}n_1(\boldsymbol{y}) - \frac{(x_1-y_1)^2(x_2-y_2)}{r^5}n_1(\boldsymbol{y}) - \frac{(x_1-y_1)(x_2-y_2)^2}{r^5}n_2(\boldsymbol{y})\right] d\boldsymbol{y}, \quad \text{(A2.7)}$$

$$J_5^{2,0}(\boldsymbol{x},\Omega_j^h) = \frac{1}{5}\int\limits_{\partial\Omega_j^h} \left[4\frac{x_1-y_1}{r^3}n_1(\boldsymbol{y}) + 2\frac{x_2-y_2}{r^3}n_2(\boldsymbol{y}) - \frac{(x_1-y_1)^3}{r^5}n_1(\boldsymbol{y}) - \frac{(x_1-y_1)^2(x_2-y_2)}{r^5}n_2(\boldsymbol{y})\right] d\boldsymbol{y}, \quad \text{(A2.8)}$$

$$J_5^{0,2}(\boldsymbol{x},\Omega_j^h) = \frac{1}{5}\int\limits_{\partial\Omega_j^h} \left[4\frac{x_2-y_2}{r^3}n_2(\boldsymbol{y}) + 2\frac{x_1-y_1}{r^3}n_1(\boldsymbol{y}) - \frac{(x_2-y_2)^3}{r^5}n_2(\boldsymbol{y}) - \frac{(x_1-y_1)(x_2-y_2)^2}{r^5}n_1(\boldsymbol{y})\right] d\boldsymbol{y}. \quad \text{(A2.9)}$$